Hindawi
Complexity
Volume 2020, Article ID 8974763, 13 pages
https://doi.org/10.1155/2020/8974763

WILEY | Hindawi

Research Article

Dynamic Complexity of a Phytoplankton-Fish Model with the Impulsive Feedback Control by means of Poincaré Map

Dezhao Li,[1] Yu Liu,[2] and Huidong Cheng [1]

[1]*College of Mathematics and System Sciences, Shandong University of Science and Technology, Qingdao, China*
[2]*College of Foreign Languages, Shandong University of Science and Technology, Qingdao 266590, Shandong, China*

Correspondence should be addressed to Huidong Cheng; chd900517@sdust.edu.cn

Received 15 January 2020; Accepted 21 March 2020; Published 15 April 2020

Academic Editor: Lingzhong Guo

The phytoplankton-fish model for catching fish with impulsive feedback control is established in this paper. Firstly, the Poincaré map for the phytoplankton-fish model is defined, and the properties of monotonicity, continuity, differentiability, and fixed point of Poincaré map are analyzed. In particular, the continuous and discontinuous properties of Poincaré map under different conditions are discussed. Secondly, we conduct the analysis of the necessary and sufficient conditions for the existence, uniqueness, and global stability of the order-1 periodic solution of the phytoplankton-fish model and obtain the sufficient conditions for the existence of the order-k ($k \geq 2$) periodic solution of the system. Numerical simulation shows the correctness of our results which show that phytoplankton and fish with the impulsive feedback control can live stably under certain conditions, and the results have certain reference value for the dynamic change of phytoplankton in aquatic ecosystems.

1. Introduction

Fisheries can provide people with quality food resources for the survival and development of human beings. Therefore, the healthy development of fishery resources is the focus of attention. If we cannot regulate the capture of fish regularly, it will lead to the depletion of fishery resources. People would be faced with increasing shortages of fish resources. Therefore, it is imperative to formulate effective fishing strategies, maintain the ecological balance of fishery resources, and protect the ecological environment [1–4].

Due to the interaction of energy conversion and the nutrient cycle between plankton and herbivores (such as fish), they play an significant role in the most terrestrial and aquatic ecological system. In [5], a phytoplankton and zooplankton model is established by the interaction of nutrients, and the dynamics properties such as limit cycle are investigated in this paper. In [6], a commercially valuable model of phytoplankton and zooplankton predation is proposed, which analyzes the stability of the equilibrium point, explores methods to maintain the ecological balance of the population at different harvest levels, and discusses the impact of selective harvesting on fisheries.

Recently, threshold state pulsed dynamic systems have been widely used [7–14]. The geometric theory of impulse dynamical system has been well-developed [15–23]. Many pulse equations have been studied which simulate the ecological processes of populations [24–32]. However, with the further development of the state feedback control model, we need more new methods to find out the complete dynamic properties and control strategies of dynamic systems and to discuss its biological significance. The primary purpose of this paper is to provide a comprehensive qualitative analysis of the global dynamics through analyzing a phytoplankton-fish model with impulse feedback control using the Poincaré map.

The central arrangement of this paper is as follows. In Section 2, we establish a phytoplankton-fish model for catching fish based on impulse feedback control. In Section 3, the Poincaré map for the phytoplankton-fish model is defined and the properties of monotonicity, continuity, and differentiability of the Poincaré map are analyzed. In Section 4, we discuss the existence, uniqueness, and global stability of the order-1 periodic solution of the model and obtain the conditions for the existence of order-k ($k \geq 2$) periodic solution of the model. In Section 5, we perform numerical simulations.

2. Model Establishment

In the ecosystem of lakes, phytoplankton is considered to be the most favorable source of food for fish or other aquatic animals. Wang et al. [33] propose a predator model of continuously harvested phytoplankton and herbivorous fish:

$$\begin{cases} \dfrac{\mathrm{d}u}{\mathrm{d}t} = ru\left(1-\dfrac{u}{k}\right) - \dfrac{\beta uv}{\alpha+u} - c_1Eu, \\ \dfrac{\mathrm{d}v}{\mathrm{d}t} = \dfrac{\beta_1 uv}{\alpha+u} - \mathrm{d}v - \dfrac{\rho uv}{\alpha+u} - c_2Ev, \end{cases} \tag{1}$$

where u and v represent the population density of phytoplankton and fish at the moment, respectively, and E is the effort for continuous harvesting. For details of other parameters, see [34–36].

System (1) shows that, without considering the number of phytoplankton and herbivore, continuous capture will lead to resource depletion. We will seek an integrated capture strategy to achieve ecological stability, for which we make the following assumption:

(i) Assuming that phytoplankton and fish stocks are evenly distributed within the lake

(ii) Let r be the intrinsic growth rate of phytoplankton, α be the absorption rate of phytoplankton by fish, β be the conversion rate of biomass, and d denote the mortality rate of fish

(iii) Formula $au/b+u$ represents the death number of fish due to the distribution of phytoplankton toxicants, where b represents semisaturation constant and a represents the rate at which phytoplankton releases toxins

Let H denote the threshold at which the fish are allowed to be caught, that is, when the density of the fish is lower than the threshold H, it is unreasonable to catch fish; however, only when the density of fish reaches, the predetermined value H can catch the fish. The amount of phytoplankton is affected when the fish is caught. The numbers of the fish and the amount of phytoplankton are updated to $v(t) - (\tau/1 + \theta v(t))$ and $u(t)(1 - (\delta u(t)/u(t) + \gamma))$, respectively.

Here, δ represents the maximum fishing rate, γ represents the half-saturation constant, τ indicates the number of phytoplankton reductions, and θ represents the morphology parameters, where $0 < \delta < 1$, $\gamma > 0$, $\tau > 0$, and $\theta > 0$ [37].

We have established the following impulse feedback control model based on the abovementioned assumptions:

$$\begin{cases} \left.\begin{aligned} &\dfrac{\mathrm{d}u}{\mathrm{d}t} = (r-\alpha v(t))u(t) \\ &\dfrac{\mathrm{d}v}{\mathrm{d}t} = \left(\beta u(t) - d - \dfrac{au(t)}{b+u(t)}\right)v(t) \end{aligned}\right\} v(t) < H, \\ \left.\begin{aligned} &u(t^+) = u(t)\left(1-\dfrac{\delta u(t)}{u(t)+\gamma}\right) \\ &v(t^+) = v(t) - \dfrac{\tau}{1+\theta v(t)} \end{aligned}\right\} v(t) = H. \end{cases} \tag{2}$$

System (2) is called a semicontinuous dynamic system [38–40].

When there is no impulse, system (2) becomes

$$\begin{cases} \dfrac{\mathrm{d}u}{\mathrm{d}t} = (r-\alpha v(t))u(t), \\ \dfrac{\mathrm{d}v}{\mathrm{d}t} = \left(\beta u(t) - d - \dfrac{au(t)}{b+u(t)}\right)v(t). \end{cases} \tag{3}$$

Lemma 1 (see [37]). *System (3) has two equilibrium points, O(0,0) and $E^*(u^*, v^*)$, where the boundary equilibrium point $(0,0)$ is the saddle point and the internal balance point (u^*, v^*) is a stable center:*

$$u^* = \frac{d+a-\beta b + \sqrt{(d+a-\beta b)^2 - 4\beta bd}}{2\beta}, \quad v^* = \frac{r}{\alpha}. \tag{4}$$

It is easy to calculate, the first integral of system (3) is

$$H(u,v) = \beta u - d\ln u - a\ln(b+u) - r\ln v + \alpha v + H_0, \tag{5}$$

where H_0 is the constant related to the initial value. For ease of expression, two isoclines are defined as

$$L_1 \colon v = \frac{r}{\alpha}; \quad L_2 \colon u = \frac{d+a-\beta b + \sqrt{(d+a-\beta b)^2 - 4\beta bd}}{2\beta}. \tag{6}$$

To study the dynamic properties of system (2), the following research methods are given.

3. Poincaré Map of System (2) and Its Properties

We intersect the dynamic properties of model (2) in $R_2^+ = \{(u,v), u \geq 0, v \geq 0\}$ based on biological significance. In order to accurately define the impulse set and phase set of the pulsed semidynamic system (2), the following set is given first:

$$\begin{aligned} \Sigma_N &= \left\{(u,v) \,\middle|\, u \geq 0, v = H - \frac{\tau}{1+\theta H}\right\}, \\ \Sigma_M &= \{(u,v) \mid u \geq 0, v = H\}. \end{aligned} \tag{7}$$

Apparently, within R_2^+, Σ_N and Σ_M represent two straight lines of the vertical v-axis, respectively, and we assume Σ_N and Σ_M intersect the line L_2 at point A^+ and point A^-, respectively, since the internal balance point E^* is the center point. According to the size of H, we can divide the pulse set and phase set into the following cases:

Case I: $H < v_*$

When $H < v_*$, the trajectory Γ_{A^+} must intersect the Σ_M at point $A_{11}(u_{11}, H)$ (see Figure 1(a)). In this case, impulse sets

$$M_1 = \{(u,v) \mid v = H, u \geq u_{11}\}, \tag{8}$$

and the corresponding phase set is

$$N_1 = \left\{(u,v) \mid v = H - \frac{\tau}{1+\theta H}, \quad u \geq u_{11}\left(1 - \frac{\delta u_{11}}{u_{11}+\gamma}\right)\right\}. \tag{9}$$

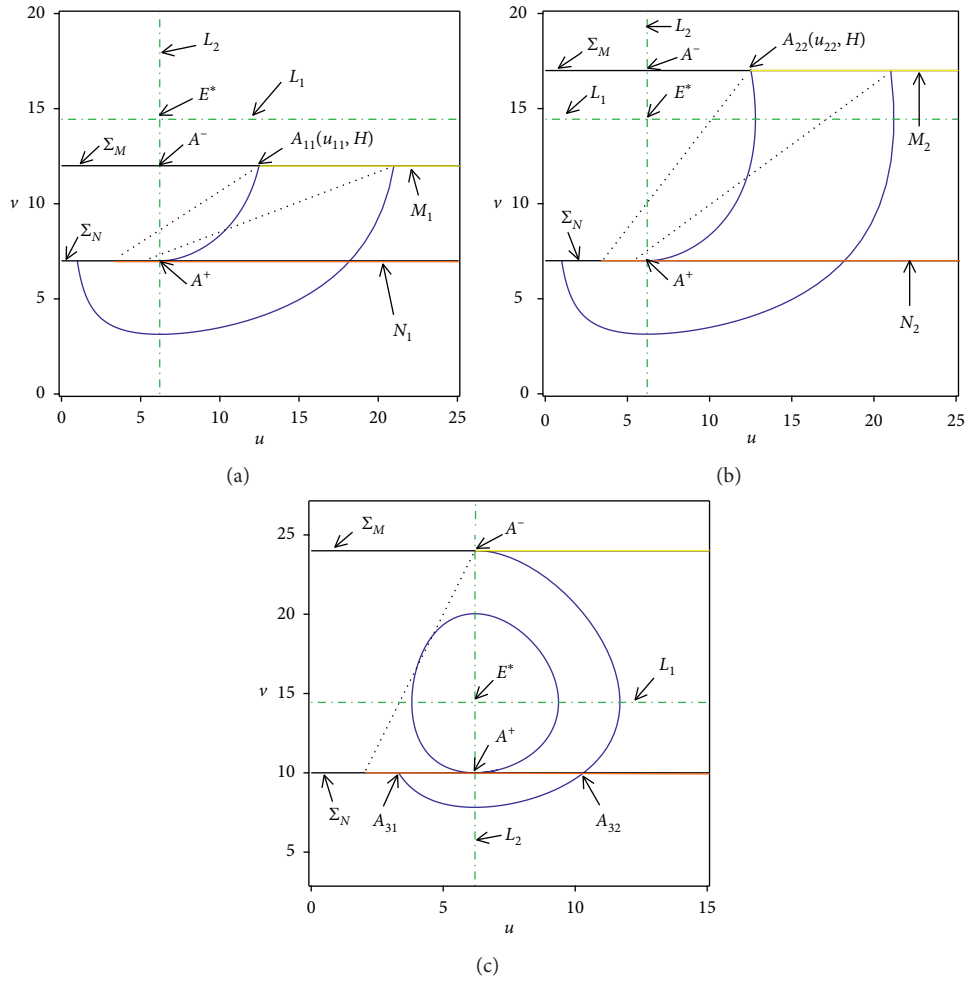

FIGURE 1: The domain of phase set and pulse set in three cases. The parameter values are as follows: $r = 1.444$, $\alpha = 0.1$, $\beta = 0.15$, $d = 0.5$, $a = 0.5$, $b = 1$, $\delta = 0.8$, and $\gamma = 1$. (a) $H = 12$, $\theta = 0.02$, and $\tau = 6.2$. (b) $H = 17$, $\theta = 0.01$, and $\tau = 11.7$. (c) $H = 24$, $\theta = 0.01$, and $\tau = 17.36$.

Case II: $H > v_*$

When $H > v_*$, if the trajectory Γ_{A^+} intersects the Σ_M at a point, we assume this intersect is $A_{22}(u_{22}, H)$ (see Figure 1(b)). In this case, the impulse set and the phase set are the same as those in Case I. It is easy to infer the impulse set

$$M_2 = \{(u, v) \mid , v = H, u \geq u_{22}\}, \tag{10}$$

and the corresponding phase set

$$N_2 = \left\{(u, v) \mid v = H - \frac{\tau}{1 + \theta H}, u \geq u_{22}\left(1 - \frac{\delta u_{22}}{u_{22} + \gamma}\right)\right\}. \tag{11}$$

If the trajectory Γ_{A^+} and Σ_M does not intersect (see Figure 1(c)), the trajectory Γ_{A^-} intersects the Σ_N at point $A_{31}(u_{31}, H - (\tau/1 + \theta H))$ and point $A_{32}(u_{32}, H - (\tau/1 + \theta H))$, respectively, where $u_{32} > u_{31}$.

In this case, the impulse set

$$M_3 = \{(u, v) \mid v = H, u \geq u^*\}, \tag{12}$$

and the corresponding phase set

$$N_3 = \left\{(u, v) \mid v = H - \frac{\tau}{1 + \theta H}, \quad u \geq u^*\left(1 - \frac{\delta u^*}{u^* + \gamma}\right)\right\}. \tag{13}$$

Based on the abovementioned discussion, we define the Poincaré map as follows.

Let

$$A_k^+ = (u_k^+, v_k^+) = \left(u_k^+, H - \frac{\tau}{1 + \theta H}\right) \in \Sigma_N, \tag{14}$$

where $0 < u_k^+ < +\infty$; the trajectory

$$\pi\left(t, t_0, \left(u_k{}^+, H - \frac{\tau}{1 + \theta H}\right)\right) \triangleq \left(u\left(t, t_0, \left(u_k{}^+, H - \frac{\tau}{1 + \theta H}\right)\right), v\left(t, t_0, \left(u_k{}^+, H - \frac{\tau}{1 + \theta H}\right)\right)\right), \tag{15}$$

which goes through point A_k^+ will reach the Σ_M at point

$$A_{k+1}(t_1, t_0, (u_{k+1}, H)) \stackrel{\Delta}{=} A_{k+1}(u_{k+1}, H), \tag{16}$$

after time t_1, and here

$$v\left(t_1, t_0, \left(u_k^+, H - \frac{\tau}{1+\theta H}\right)\right) = H. \tag{17}$$

Then, there is

$$u_{k+1}^+ = u\left(t_1, t_0, \left(u_k^+, H - \frac{\tau}{1+\theta H}\right)\right) \triangleq u\left(u_k^+, H - \frac{\tau}{1+\theta H}\right) \triangleq = P(u_k^+), \tag{18}$$

which indicates that the ordinate u_{k+1}^+ is determined by u_k^+.

Since point A_{k+1} is on the impulse set, A_{k+1} jumps to point

$$A_{k+1}^+ = \left(u_{k+1}^+, H - \frac{\tau}{1+\theta H}\right), \tag{19}$$

where

$$u_{k+1}^+ = \left(1 - \frac{\delta u_{k+1}}{u_{k+1}+\gamma}\right)u_{k+1} = \left(1 - \frac{\delta P(u_k^+)}{P(u_k^+)+\gamma}\right)P(u_k^+) \triangleq = G_m(u_k^+). \tag{20}$$

Consider the scalar differential equation of model (3):

$$\begin{cases} \dfrac{du}{dv} = \dfrac{(r-\alpha v)u}{(\beta u - d - au/b + u)v} \triangleq w(u,v), \\ u\left(H - \dfrac{\tau}{1+\theta H}\right) = u_0^+. \end{cases} \tag{21}$$

Let $v_0^+ = H - (\tau/1+\theta H)$ and $u_0^+ = S$, then we have (u_0^+, v_0^+) in Σ_N.

We define

$$\mu(x) = u\left(x; H - \frac{\tau}{1+\theta H}, S\right) \triangleq \mu(x,S), \quad H - \frac{\tau}{1+\theta H} \le x \le H. \tag{22}$$

According to model (21),

$$\mu(x,S) = S + \int_{H-(\tau/1+\theta H)}^{x} \omega(s, u(s,S))ds. \tag{23}$$

From (20) and (23), the Poincaré map expression of system (2) is

$$G_m(S) = \left(1 - \frac{\delta\mu(H - \tau/1+\theta H, S)}{\mu(H - \tau/1+\theta H, S)+\gamma}\right)\mu\left(H - \frac{\tau}{1+\theta H}, S\right). \tag{24}$$

The properties of the Poincaré map $G_m(s)$ is discussed below.

Theorem 1. *Let $H < v^*$, trajectory Γ_{A^+} intersects with line Σ_M at point $A_{11}(u_{11}, H)$ and point $A_{12}(u_{12}, H)$, respectively, where $u_{11} > u_{12}$. Poincare map $G_m(s)$ has the following properties:*

(i) The domain of $G_m(s)$ is $(0, +\infty)$, $G_m(s)$ is monotonically decreasing on $(0, u^*]$, and monotonically increasing on $(u^*, +\infty)$.

(ii) $G_m(s)$ is continuously differentiable on $(0, +\infty)$.

(iii) When $G_m(u^*) > u^*$, there is a unique fixed point on $(u^*, +\infty)$ (see Figure 2(b)). When $G_m(u^*) < u^*$, there is a unique fixed point on $(0, u^*)$ (see Figure 2(a)). When $G_m(u^*) = u^*$, u^* is the fixed point of $G_m(s)$.

Proof

(i) Since $E^*(u^*, v^*)$ is the center point and $H < v^*$, take any point $A_k^+(u_k^+, v_k^+)$ on Σ_N, and the trajectory of point A_k^+ will reach the impulse set M_1 at point $A_{k+1}(u_k, H)$, so the domain of $G_m(s)$ is $(0, +\infty)$.

For any $u_{k_1}^+, u_{k_2}^+ \in [u^*, +\infty)$ and $u_{k_1}^+ < u_{k_2}^+$, from the uniqueness of the solution of the differential equation, it can be known that

$$\mu\left(u_{k_1}^+, v\right) < \mu\left(u_{k_2}^+, v\right), \quad H - \frac{\tau}{1+\theta H} \le v \le H, \tag{25}$$

and by the definition of the Poincaré map we can get $G_m(u_{k_1}^+) < G_m(u_{k_2}^+)$. Therefore, $G_m(s)$ is monotonically increasing on $[u^*, +\infty)$.

When $u_{k_1}^+, u_{k_2}^+ \in (0, u^*)$, where $u_{k_1}^+ < u_{k_2}^+$. The trajectories start from point $A_{k_1}^+(u_{k_1}^+, H - (\tau/1+\theta H))$, and point $A_{k_2}^+(u_{k_2}^+, H - (\tau/1+\theta H))$ will pass through the isocline L_2 and intersect the set Σ_N at point $A_{k_{11}}^+(u_{k_{11}}^+, H - (\tau/1+\theta H))$ and point $A_{k_{21}}^+(u_{k_{21}}^+, H - (\tau/1+\theta H))$, respectively, where $u_{k_{i1}}^+ (i = 1, 2) \in [u^*, +\infty)$ and $u_{k_{11}}^+ > u_{k_{21}}^+$. It can be seen from the uniqueness of the solution of the differential equation that $G_m(u_{k_{11}}^+) > G_m(u_{k_{21}}^+)$ because $G_m(u_{k_{11}}^+) = G_m(u_{k_1}^+)$ and $G_m(u_{k_{21}}^+) = G_m(u_{k_2}^+)$, so $G_m(u_{k_1}^+) > G_m(u_{k_2}^+)$; therefore, $G_m(s)$ is monotonically decreasing on $(0, u^*)$.

Note 1. Because $G_m(s)$ is monotonically decreasing on $(0, u^*]$ and monotonically increasing on $(u^*, +\infty)$, it is easy to know that $G_m(s) \ge G_m(u^*)$ is true for any $s \in (0, +\infty)$, and $G_m(s) = G_m(u^*)$ if and only if $s = u^*$.

(ii) It is easy to know that $w(u, v)$ is continuously differentiable in the first quadrant from (21), and from the continuous differentiability theorem of differential equations, that is, the Cauchy and Lipschitz theorem with parameters, we know that the Poincare map $G_m(s)$ is continuously differentiable in the first quadrant.

(iii) Considering the Poincaré map at the position of image $G_m(u^*)$ of u^*, there are three cases:

(a) When $G_m(u^*) = u^*$, then u^* is the fixed point of function $G_m(s)$.

(b) When $G_m(u^*) > u^*$, that is, $G_m(u^*) - u^* > 0$ because $0 < \delta < 1$, then

$$\lim_{s \longrightarrow \infty} G_m(s) = s\left(1 - \frac{\delta s}{s+\gamma}\right) = s\left(1 - \delta - \frac{\delta\gamma}{s+\gamma}\right) < s(1-\delta) < s. \tag{26}$$

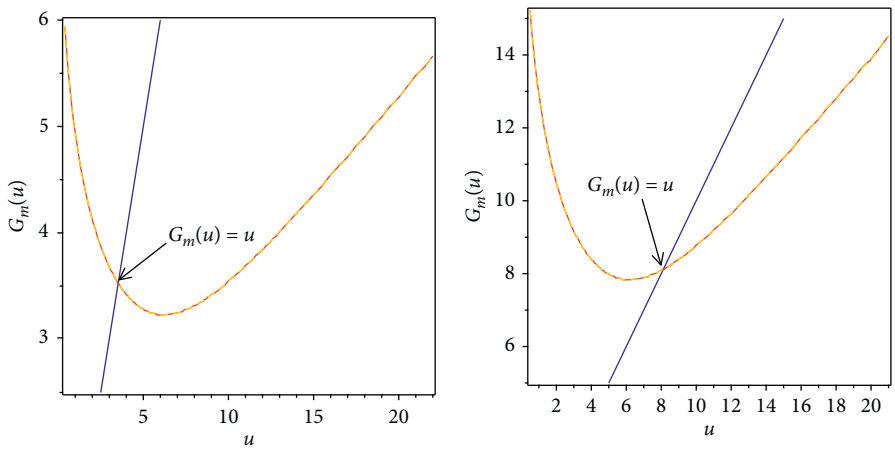

FIGURE 2: The Poincaré map $G_m(u)$ related to the impulsive point series u. The parameter values are as follows: $r = 1.444$, $\alpha = 0.1$, $\beta = 0.15$, $d = 0.5$, $a = 0.5$, $b = 1$, $\delta = 0.8$, and $\gamma = 1$. (a) $H = 12$, $\theta = 0.02$, and $\tau = 6.2$. (b) $H = 15$, $\theta = 0.01$, and $\tau = 15.4$.

That is, $\lim_{s\longrightarrow\infty} G_m(s) - s < 0$. So, it has at least one $\tilde{u} \in (u^*, +\infty)$ satisfies $G_m(\tilde{u}) = \tilde{u}$, according to the continuous differentiable of the closed interval.

(c) When $G_m(u^*) < u^*$, let $G_m(u^*) = u_1 < u^*$, we know that $G_m(s)$ is monotonically decreasing on $(0, u^*]$, so $G_m(u_1) > G_m(u^*) = u_1$, and because $G_m(u^*) < u^*$, so there is at least one $\tilde{u} \in (u_1, u^*)$ which satisfies $G_m(\tilde{u}) = \tilde{u}$, according to the continuous differentiable of the closed interval.

In conclusion, $G_m(s)$ has at least one fixed point. Then, we prove the fixed point is unique.

We assume that system (2) has two fixed points, $\tilde{u}_1$ and $\tilde{u}_2$, that is to say $G_m(\tilde{u}_1) = \tilde{u}_1$ and $G_m(\tilde{u}_2) = \tilde{u}_2$. Let $\tilde{u}_1 < \tilde{u}_2$, we define

$$d_{\tilde{u}_1\tilde{u}_2}(u) = u(v, \tilde{u}_2) - u(v, \tilde{u}_1), \quad H - \frac{\tau}{1+\theta H} \le v \le H. \tag{27}$$

Then, take the derivative of the abovementioned formula:

$$d'_{\tilde{u}_1\tilde{u}_2}(u) = u'(v, \tilde{u}_2) - u'(v, \tilde{u}_1) = \frac{r - \alpha v}{v}\left[\frac{\tilde{u}_2}{\beta\tilde{u}_2 - d - (a\tilde{u}_2/b + \tilde{u}_2)} - \frac{\tilde{u}_1}{\beta\tilde{u}_1 - d - (a\tilde{u}_1/b + \tilde{u}_1)}\right]. \tag{28}$$

Let

$$g(u) = \frac{u}{\beta u - d - (au/b + u)}. \tag{29}$$

Then,

$$g'(u) = \frac{-d - a(u/b + u)^2}{(\beta u - d - (au/b + u))^2} < 0, \tag{30}$$

so

$$g(\tilde{u}_2) < g(\tilde{u}_1), \tag{31}$$

that is,

$$d'_{\tilde{u}_1\tilde{u}_2}(u) < 0, \tag{32}$$

and

$$d_{\tilde{u}_1\tilde{u}_2}\left(H - \frac{\tau}{1+\theta H}\right) > d_{\tilde{u}_1\tilde{u}_2}(H). \tag{33}$$

From system (2),

$$\begin{aligned}
\tilde{u}_1 &= \mu(\tilde{u}_1)\left(1 - \frac{\delta\mu(\tilde{u}_1)}{\mu(\tilde{u}_1) + \gamma}\right) \\
&= \mu(\tilde{u}_1)\left(1 - \delta + \frac{\delta\gamma}{\mu(\tilde{u}_1) + \gamma}\right) \\
&= \left[\mu(\tilde{u}_2) - d_{\tilde{u}_1\tilde{u}_2}(H)\right]\left(1 - \delta + \frac{\delta\gamma}{\mu(\tilde{u}_1) + \gamma}\right) \\
&= \mu(\tilde{u}_2)\left(1 - \delta + \frac{\delta\gamma}{\mu(\tilde{u}_1) + \gamma}\right) - d_{\tilde{u}_1\tilde{u}_2}(H)\left(1 - \delta + \frac{\delta\gamma}{\mu(\tilde{u}_1) + \gamma}\right) \\
&> \mu(\tilde{u}_2)\left(1 - \delta + \frac{\delta\gamma}{\mu(\tilde{u}_2) + \gamma}\right) - \frac{\tilde{u}_1 d_{\tilde{u}_1\tilde{u}_2}(H)}{\mu(\tilde{u}_1)} \\
&= \tilde{u}_2 - \frac{\tilde{u}_1 d_{\tilde{u}_1\tilde{u}_2}(H)}{\mu(\tilde{u}_1)},
\end{aligned} \tag{34}$$

that is,

$$\frac{\tilde{u}_1 d_{\tilde{u}_1\tilde{u}_2}(H)}{\mu(\tilde{u}_1)} > \tilde{u}_2 - \tilde{u}_1 = d_{\tilde{u}_1\tilde{u}_2}\left(H - \frac{\tau}{1+\theta H}\right). \tag{35}$$

It is easy to know that $(\tilde{u}_1/\mu(\tilde{u}_1)) < 1$ if $H < v^*$, so

$$d_{\tilde{u}_1\tilde{u}_2}(H) > \frac{\tilde{u}_1 d_{\tilde{u}_1\tilde{u}_2}(H)}{\mu(\tilde{u}_1)} > d_{\tilde{u}_1\tilde{u}_2}\left(H - \frac{\tau}{1+\theta H}\right). \tag{36}$$

It is contradictory with $d_{\tilde{u}_1\tilde{u}_2}(H - (\tau/1+\theta H)) > d_{\tilde{u}_1\tilde{u}_2}(H)$, so the fixed point is unique.

Note 2. When $H > v^*$ and trajectory Γ_{A^+} is an intersect to line Σ_M, the Poincare map $G_m(s)$ of system (2) has similar properties to case (a). □

Theorem 2. *Let $H > v^*$, and trajectory Γ_{A^+} does not intersect line Σ_M and trajectory Γ_{A^-} intersects the straight line Σ_N at point $A_{31}(u_{31}, H - (\tau/1 + \theta H))$ and point $A_{32}(u_{32}, H - (\tau/1 + \theta H))$, respectively, where $u_{32} > u_{31}$. Poincare map $G_m(s)$ has the following properties:*

(i) The domain of $G_m(s)$ is $(0, u_{31}] \cup [u_{32}, +\infty)$, where $G_m(s)$ is monotonically decreasing on $(0, u_{31}]$ and monotonically increasing on $[u_{32}, +\infty)$.

(ii) $G_m(s)$ is continuously differentiable on $(0, u_{31}]$ and $[u_{32}, +\infty)$, respectively.

(iii) When $G_m(u_{31}) \le u_{31}$, there is a unique fixed point on $(0, u_{31}]$ (see Figure 3(a)). When $G_m(u_{31}) > u_{31}$, there is no fixed point (see Figure 3(b)).

Proof

(i) Since $E^*(u^*, v^*)$ is the center point. If $H > v^*$ and trajectory Γ_{A^+} does not intersect line Σ_M, trajectory Γ_{A^-} intersects the straight line Σ_N at two points, that is, $A_{31}(u_{31}, H - (\tau/1 + \theta H))$ and $A_{32}(u_{32}, H - (\tau/1 + \theta H))$, respectively, where $u_{32} > u_{31}$, then we take any point $A_k^+(u_k^+, v_k^+)$ in Σ_N. If $u_k^+ \in (0, u_{31}] \cup [u_{32}, +\infty)$, the trajectory of point A_k^+ will reach the impulse set M_3 at point $A_{k+1}(u_k, H)$, if $u_k^+ \in (u_{31}, u_{32})$ the trajectory of point A_k^+ has no intersection with the impulse set M_3. So, the domain of $G_m(s)$ is $(0, u_{31}] \cup [u_{32}, +\infty)$.

For any $u_{k_1}^+, u_{k_2}^+ \in [u_{32}, +\infty)$ and $u_{k_1}^+ < u_{k_2}^+$, from the uniqueness of the solution of the differential equation, it can be known that

$$\mu\left(u_{k_1}^+, v\right) < \mu\left(u_{k_2}^+, v\right), \quad H - \frac{\tau}{1 + \theta H} \le v \le H, \tag{37}$$

and by the definition of the Poincare map we get $G_m(u_{k_1}^+) < G_m(u_{k_2}^+)$. Therefore, $G_m(s)$ is monotonically increasing on $[u_{32}, +\infty)$.

When $u_{k_1}^+, u_{k_2}^+ \in (0, u_{31}]$, and where $u_{k_1}^+ < u_{k_2}^+$. The trajectories start from point $A_{k_1}^+(H - (\tau/1 + \theta H), u_{k_1}^+)$ and point $A_{k_2}^+(H - (\tau/1 + \theta H), u_{k_2}^+)$ will pass through the isocline L_2 which intersects the Σ_N at point $A_{k_{11}}^+(H - (\tau/1 + \theta H), u_{k_{11}}^+)$ and point $A_{k_{21}}^+(H - (\tau/1 + \theta H), u_{k_{21}}^+)$, respectively. Then, $u_{k_{i1}}^+ (i = 1, 2) \in [u_{32}, +\infty)$ and $u_{k_{11}}^+ > u_{k_{21}}^+$. It can be seen from the uniqueness of the solution of the differential equation that $G_m(u_{k_1}^+) > G_m(u_{k_2}^+)$; therefore, $G_m(s)$ is monotonically decreasing on $(0, u_{31}]$.

(ii) From (21), we can know that $w(u, v)$ is continuously differentiable in the first quadrant; from the continuous differentiability theorem of differential equations, that is, the Cauchy and Lipschitz theorem with parameters, we know that the $G_m(s)$ is continuously differentiable on $(0, u_{31}]$ and $[u_{32}, +\infty)$, respectively.

(iii) Considering the Poincare map at the position of image $G_m(u_{31})$ of u_{31}, there are two cases:

(a) When $G_m(u_{31}) \le u_{31}$ (see Figure 3(a)), we assume $G_m(u_{31}) = u_1 \le u_{31}$, and we know that $G_m(s)$ is monotonically decreasing on $(0, u_{31}]$, so $G_m(u_1) \ge G_m(u_{31}) = u_1$, and because $G_m(u_{31}) \le u_{31}$, so there is a point $\tilde{u} \in (u_1, u_{31}]$, and it satisfies $G_m(\tilde{u}) = \tilde{u}$, according to the continuous differentiability of the closed interval.

(b) When $G_m(u_{31}) > u_{31}$ (see Figure 3(b)), there is no $\tilde{u} \in (0, u_{31}]$ which satisfies $G_m(\tilde{u}) = \tilde{u}$.

For any $u_k \in (u_{32}, +\infty)$, the trajectory of point $A_k(u_k, H - (\tau/1 + \theta H))$ is tangent to the straight line Σ_M at point $A_k^+(u_k^+, H)$; $A_k^+(u_k^+, H - (\tau/1 + \theta H))$ will be pulsed to $A_{k+1}(u_{k+1}, H - (\tau/1 + \theta H))$. Easy to get $u_{k+1} < u_k^+ < u_k$, that is, $u_{k+1} \ne u_k$, so there is no $u \in (u_{32}, +\infty)$ and satisfies $G_m(\tilde{u}) = \tilde{u}$.

In a word, when $G_m(u_{31}) \le u_{31}$, there is a unique fixed point on $(0, u_{31}]$. When $G_m(u_{31}) > u_{31}$, there is no fixed point. □

4. The Order-k ($k \ge 1$) Periodic Solution of the Semicontinuous Dynamic System (2) and Its Stability

From Theorem 1, we know that system (2) has a unique fixed point under certain conditions. That is, system (2) has a unique order-1 periodic solution, and the following are the dynamic properties of system (2).

Theorem 3. *$H < v^*$ and $G_m(u^*) > u^*$ are established, then the order-1 periodic solution of system (2) is globally asymptotically stable.*

Proof. From (iii) of Theorem 1, we know that when $G_m(u^*) > u^* \otimes$, $G_m(s)$ has a unique fixed point $\tilde{u}$ on $(u^*, +\infty)$, i.e., $G_m(\tilde{u}) = \tilde{u}$. For any point $p_0^+(H - (\tau/1 + \theta H), u_0^+)$ in Σ_N, where $u_0^+ > u^*$, the trajectory of the point p_0^+ will intersect the impulse set, then reach the point $p_1^+(H - (\tau/1 + \theta H), u_1^+)$, which is $G_m(u_0^+) = u_1^+$, repeating the abovementioned process:

$$G_m\left(G_m\left(u_0^+\right)\right) = G_m^2\left(u_0^+\right), \tag{38}$$

that is,

$$G_m\left(u_1^+\right) = u_2^+. \tag{39}$$

Furthermore,

$$u_n^+ = G_m^n\left(u_0^+\right), \quad n = 1, 2, \ldots. \tag{40}$$

The following two cases are discussed below according to the size of u_0^+:

1) When $u^* < u_0^+ \le \tilde{u}$, since $G_m(u^*) > u^*$ and $G_m(s)$ is monotonously increasing on $(u^*, +\infty)$, let $G_m(u_i^+) = u_{i+1}^+$, then

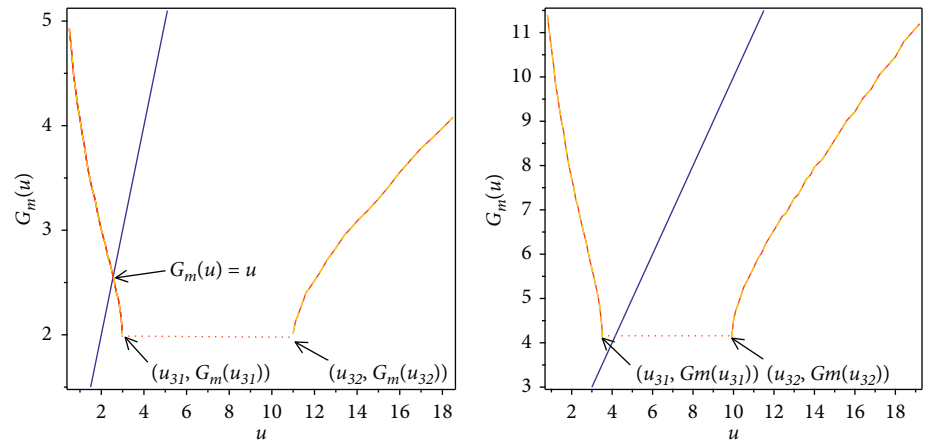

FIGURE 3: The Poincaré map $G_m(u)$ related to the impulsive point series u. The parameter values are as follows: $r = 1.444$, $\alpha = 0.1$, $\beta = 0.15$, $d = 0.5$, $a = 0.5$, $b = 1$, $\delta = 0.8$, and $\gamma = 1$. (a) $H = 18$, $\theta = 0.02$, and $\tau = 16.2$. (b) $H = 24$, $\theta = 0.01$, and $\tau = 17.36$.

$$u_0^+ < G_m(u_0^+) = u_1^+ \le G_m(\tilde{u}) = \tilde{u},$$
$$u_0^+ < G_m(u_0^+) < G_m(u_1^+) = {G_m}^2(u_0^+) \le G_m(\tilde{u}) = \tilde{u}. \tag{41}$$

Repeating the abovementioned process, we can obtain

$$u_0^+ < G_m(u_0^+) < \cdots < G_m^n(u_0^+) < \cdots < \tilde{u}. \tag{42}$$

From the monotonous boundedness of the sequence, we can obtain

$$\lim_{n\longrightarrow+\infty} {G_m}^n(u_0^+) = \tilde{u}. \tag{43}$$

(2) When $\tilde{u} < u_0^+ < +\infty$, from the known conditions,

$$\tilde{u} = G_m(\tilde{u}) < G(u_0^+). \tag{44}$$

Furthermore,

$$\tilde{u} = G_m(\tilde{u}) < {G_m}^2(u_0^+) < G(u_0^+). \tag{45}$$

By mathematical induction,

$$\tilde{u} = G_m(\tilde{u}) < \cdots < {G_m}^n \in (u_0^+) < G_m^{n-1}(u_0^+) < \cdots. \tag{46}$$

Thus,

$$\lim_{n\longrightarrow+\infty} G_m^n(u_0^+) = \tilde{u}. \tag{47}$$

(3) When $0 < u_0^+ < u^*$, since $G_m(u^*) > u^*$ and $G_m(s)$ is monotonously decreasing on $(0, u^*)$, so for any $u_0^+ \in (0, u^*)$ there is $G_m(u_0^+) > G_m(u^*) > u^*$. So, we can conclude that $G_m(u_0^+) > u^*$, and we can convert this to two cases based on the size of $G_m(u_0^+)$. When $u^* < G_m(u_0^+) < \tilde{u}$, this is the same as case (1) above; when $G_m(u_0^+) > \tilde{u}$, this is the same as case (2) above. In both cases,

$$\lim_{n\longrightarrow+\infty} G_m^n(u_0^+) = \tilde{u}. \tag{48}$$

The order-1 periodic solution of system (2) is globally asymptotically stable. □

Theorem 4. *When $H < v^*$, $G_m(u^*) < u^*$ and $G_m^2(u^*) < u^*$ are true, and then the semicontinuous dynamical system (2) has a stable order-1 periodic solution or order-2 periodic solution.*

Proof. Take a point $p_0^+(u_0^+, H - (\tau/1 + \theta H))$ on the phase set, here $u_0^+ > 0$, since E^* is the center of system (2). The trajectory that goes through point ${p_0}^+$ must intersect (Tex translation failed) at point $p_1(u_1, H)$, where $u_1 = \mu(u_0^+, H)$. p_1 will reach point $p_1^+(u_1^+, H - (\tau/1 + \theta H))$ by an impulse, so $G_m(u_0^+) = u_1^+$, repeating this process to get the sequence

$$u_n^+ = G_m^n(u_0^+) = G_m\left(G_m^{n-1}(u_0^+)\right), \quad (n = 1, 2\ldots), \tag{49}$$

When $u^* \le u_0^+ < +\infty$, we can know that $G_m(s)$ is monotonically increasing on $[u^*, +\infty)$ and there is no fixed point on $[u^*, +\infty)$ from (i) of Theorem 1. Therefore, there must be a positive integer i, which satisfies

$$u_{i-1}^+ = G_m(u_{i-2}^+) < u^*,$$
$$u_i^+ = G_m(u_{i-1}^+) < G_m(u^*) < u^*. \tag{50}$$

When $0 < u_0^+ < u^*$, the trajectory through the initial point $p_0^+(u_0^+, H - (\tau/1 + \theta H))$ will pass through the isocline L_2 and intersects (Tex translation failed) at point $p_0'(u_0', H - (\tau/1 + \theta H))$, where $0 < u_0' < u^*$; this translates into the abovementioned situation.

This means that, for any $u_0^+ \in (0, +\infty)$, there is always be a positive integer i which satisfies

$$G_m(u^*) < G_m^i(u_0^+) < u^* \quad (i \ge 1). \tag{51}$$

So, we only need to take account of the initial point $p_0^+(u_0^+, H - (\tau/1 + \theta H))$, where $u^* \le u_0^+ < G_m(u^*)$. Since $G_m(s)$ is monotonically decreasing on $[G_m(u^*), u^*]$, so

$$G_m[G_m(u^*), u^*] \subset [G_m(u^*), u^*]. \tag{52}$$

Let $G_m(u_0^+) \neq u_0^+$ and $G_m^2(u_0^+) \neq u_0^+$, that is, the trajectory with the initial point p_0^+ is not the order-1 periodic solution or order-2 periodic solution of system (2). We consider the following four situations:

Case I: $u^* \geq u_0^+ > {G_m}^2(u_0^+) > G_m(u_0^+) \geq G_m(u^*)$.

According to the monotonicity of the Poincare map,

$$u_2^+ = G_m(u_1^+) > G_m(u_2^+) = u_3^+ > G_m(u_0^+) = u_1^+. \quad (53)$$

Furthermore,

$$u_4^+ = G_m(u_3^+) < G_m(u_0^+) = u_0^+. \quad (54)$$

Thus, there is

$$u^* \geq u_0^+ > u_2^+ > u_4^+ > u_3^+ > u_1^+ \geq G_m(u^*). \quad (55)$$

Proved by mathematical induction,

$$\begin{aligned} u^* \geq u_0^+ > u_2^+ > \cdots > u_{2n}^+ > u_{2n+2}^+ > \cdots > u_{2n+1}^+ \\ > u_{2n-1}^+ > \cdots > u_1^+ \geq G_m(u^*). \end{aligned} \quad (56)$$

Case II: $u^* \geq u_1^+ > u_0^+ > u_2^+ \geq G_m(u^*)$.

Because $G_m(s)$ is monotonically decreasing on $[G_m(u^*), u^*]$. We can obtain

$$\begin{aligned} u_3^+ = G_m(u_2^+) > G_m(u_0^+) = u_1^+ > G_m(u_1^+) = u_2^+, \\ u_4^+ = G_m(u_3^+) < G_m(u_1^+) = u_2^+ < G_m(u_2^+) = u_3^+. \end{aligned} \quad (57)$$

Then,

$$u^* \geq u_3^+ > u_1^+ > u_0^+ > u_2^+ > u_4^+ \geq G(u^*), \quad (58)$$

so

$$\begin{aligned} u^* \geq \cdots > u_{2n+1}^+ > u_{2n-1}^+ > \cdots > u_3^+ > u_1^+ > u_0^+ \\ > u_2^+ > u_4^+ > \cdots > u_{2n}^+ > \cdots \geq G(u^*). \end{aligned} \quad (59)$$

Case III: $u^* \geq u_1^+ > u_2^+ > u_0^+ \geq G_m(u^*)$. In the same way, we can deduce

$$\begin{aligned} u^* \geq u_1^+ > u_3^+ > \ldots > u_{2n-1}^+ > \ldots > u_{2n+1}^+ > u_{2n}^+ \\ > \ldots > u_2^+ > u_0^+ \geq G_m(u^*). \end{aligned} \quad (60)$$

Case IV: $u^* \geq u_2^+ > u_0^+ > u_1^+ \geq G_m(u^*)$.

We can perform the procedure similar to Case I, which can yield\

$$\begin{aligned} G_m(u^*) \leq u_{2n+1}^+ < u_{2n-1}^+ < \cdots < u_1^+ < u_0^+ \\ < u_2^+ < \cdots < u_{2n}^+ < u_{2n+1}^+ < \cdots \leq u^*. \end{aligned} \quad (61)$$

Considering Cases I and III, there must exist $\tilde{u} \in (u^*, G_m(u^*))$ so that

$$\lim_{n\longrightarrow\infty} {u_{2n}}^+ = \lim_{n\longrightarrow\infty} {u_{2n-1}}^+ = \tilde{u}, \quad (62)$$

which means that system (2) has a stable order-1 periodic solution.

For Cases I and IV, there are two points $\tilde{u_1} \neq \tilde{u_2}$ and

$$\begin{aligned} \lim_{n\longrightarrow\infty} {u_{2n-1}}^+ = \tilde{u}_1, \\ \lim_{n\longrightarrow\infty} {u_{2n}}^+ = \tilde{u}_2. \end{aligned} \quad (63)$$

This shows that system (2) has a stable order-2 periodic solution with the initial points $(\tilde{u_1}, H - (\tau/1 + \theta H))$ and $(\tilde{u_2}, H - (\tau/1 + \theta H))$.

Theorem 4 illustrates that system (2) has a stable order-1 or order-2 periodic solution under certain conditions. However, sufficient and necessary conditions for global stability are not given. Then, we give below theorem. □

Theorem 5. *Let $H_1 < v^*$ and $G_m(u^*) < u^*$, then the necessary and sufficient conditions for the global stability of the order-1 periodic solution of system (2) is $G_m^2(u^+) < u^+$, for any $u^+ \in (0, u^*]$.*

Proof. Sufficiency: It can be seen from Theorem 4 that when $G_m(u^*) < u^*$, there exists $\tilde{u} \in (G_m(u^*), u^*)$ which satisfies $G_m(\tilde{u}) = \tilde{u}$.

For any $u^+ \in (\tilde{u}, u^*)$, let $u_1^+ = G_m(u^+)$ and $u_2^+ = G_m(u_1^+) = G_m^2(u^+)$ because of $G_m^2(u^+) < u^+ < u^*$, and from the monotonicity of $G_m(u)$, we can get $\tilde{u} > u_1^+ > G_m(u^*)$; furthermore, $u^* > u_2^+ > u_4^+ > \tilde{u} > u_3^+ > u_1^+ > G_m(u^*)$, so $u^* > u_{2n}^+ > \tilde{u} > u_{2n+1}^+ > G_m(u^*)$.

By the monotonic boundness of the sequence,

$$\lim_{n\longrightarrow\infty} {u_{2n}}^+ = \lim_{n\longrightarrow\infty} {u_{2n+1}}^+ = \tilde{u}. \quad (64)$$

Therefore, the order-1 periodic solution of system (2) is globally asymptotically stable.

Necessity:

We assume that the order-1 periodic solution of system (2) is globally asymptotically stable. Then, the following part proves that $G_m^2(u^+) < u^+$ is right for any $u^+ \in [\tilde{u}, u^*]$, which is proved by the counterevidence method below.

If $G_m^2(u^+) < u^+$ is not true for any $u^+ \in [\tilde{u}, u^*]$, then there exists a maximum $u_0 \in [\tilde{u}, u^*]$, which satisfies ${G_m}^2(u_0) \geq u_0$. For any $\varepsilon > 0$, there exist u_1 and $G_m^2(u_1) < u_1$, which is true for any $\tilde{u} - \varepsilon < u_1 < \tilde{u} + \varepsilon$ from Theorem 4. From the continuity of $G_m^2(u)$ on the interval $[u_0, u_1]$, it follows that there is at least one number $\vec{u} \in [u_0, u_1]$ and ${G_m}^2(\vec{u}) = \vec{u}$, which indicate that the trajectory with $(\vec{u}, H - (\tau/1 + \theta H))$ as the initial point is the order-2 periodic solution, and this is contradictory. □

Theorem 6. *If $G_m(u^*) < u^*$ and there exist $u_m^+ = min\{u^+: G_m(u^+) = u^*\}$, when $G_m^2(u^*) < u_m^+$, then system (2) has an order-3 periodic solution.*

Proof. If $G_m(u^*) < u^*$, there is a unique order-1 periodic solution in $(G_m(u^*), u^*)$, i.e., $G_m(\tilde{u}) = \tilde{u}$, where $\tilde{u} \in (G_m(u^*), u^*)$. Since the Poincare map is continuous over the closed interval $(0, \tilde{u}]$, and $G_m(\tilde{u}) = \tilde{u}$, then there exist $u_m^+ \in (0, \tilde{u})$ and $G_m(u_m^+) = u^*$. Furthermore, $G_m^3(u_m^+) = G_m^2(u^*) < u_m^+$; on the contrary, $\lim_{x\longrightarrow 0} G_m^3(x) > x$; according to the nature of the continuous function on the closed interval, at least one value of $\vec{u}$ satisfies ${G_m}^3(\vec{u}) = \vec{u}$. This means

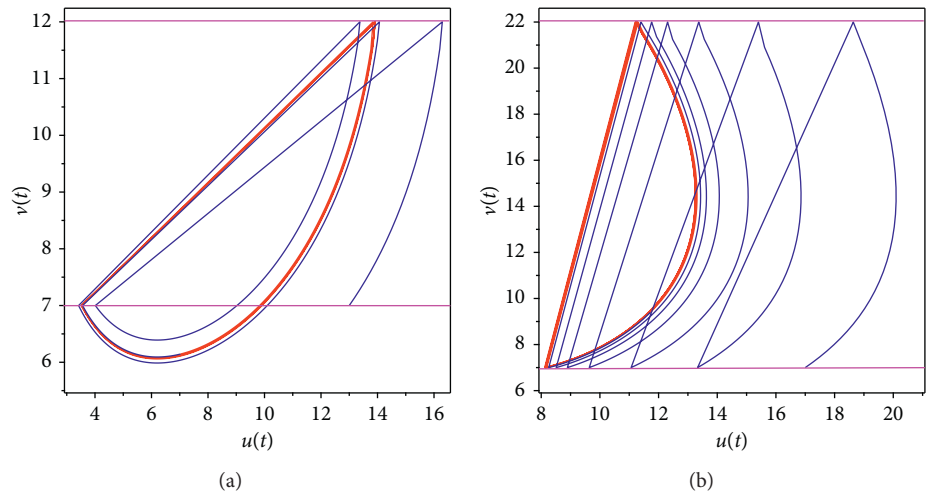

Figure 4: (a) The path curve of Figure 2(a) starting from the points (13,7); $H = 12$, $\theta = 0.02$, and $\tau = 6.2$. (b) The path curve of Figure 2(b) starting from the points (17,7), $H = 22$, $\theta = 0.01$, and $\tau = 17.36$. The parameters fixed as $r = 1.444$, $\alpha = 0.1$, $\beta = 0.15$, $d = 0.5$, $a = 0.5$, $b = 1$, $\delta = 0.8$, and $\gamma = 1$.

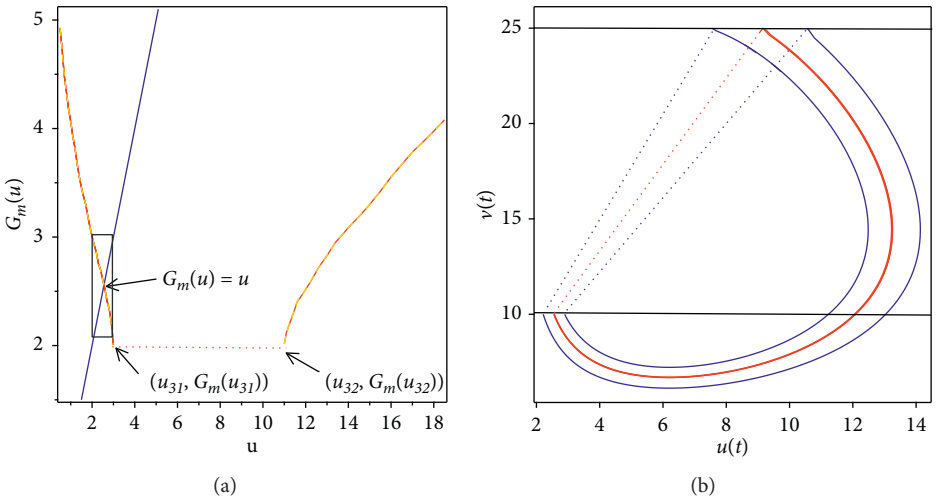

Figure 5: The positions of the order-1 periodic solution and order-2 periodic solution were found in the case of Figure 3(a).

that system (3) has an order-3 periodic solution with an initial point of $(\vec{u}, H - (\tau/1 + \theta H))$.

In a similar way, if $G_m^{k-1}(u^*) < u_m^+$, where $G_m(u_m^+) = u^*$, then system (2) has an order-k $(k \geq 2)$ periodic solution. □

5. Simulations

Figures 4(a) and 4(b), respectively, show the order-1 periodic solutions simulated under the two conditions of Figures 2(a) and 2(b), in which the blue line represents the trajectory when the order periodic solution is not reached and the red line represents the trajectory when the order periodic solution is reached. This suggests that populations of phytoplankton and fish can be kept within a stable range with the impulsive feedback control.

We simulated the order-1 periodic solution and order-2 periodic solution in the case of Figure 3(a) (see Figure 5). In the simulated Poincare map, we found the order-1 periodic solution (the intersection point of the red and yellow line and blue line in Figure 5(a)) and the order-2 periodic solution (the intersection point of the black line and red and yellow line in Figure 5(a)). Figure 5(b) shows the motion trajectories of the order-1 periodic solution and the order-2 periodic solution, in which the blue line is the motion trajectory of the order-2 periodic solution and the red and yellow line is the motion trajectory of the order-1 periodic solution.

Figures 6(a) and 6(b) are schematic diagrams of the number of phytoplankton and the number of fishes and time t in the order-2 periodic solution in Figure 5(b), respectively. Figures 6(c) and 6(d) are schematic diagrams of the planktonic quantity and the fish quantity and time t in the order-1 periodic solution in Figure 5(b), respectively. As it is revealed in the figure, the number of fish in the order-2 periodic solution and the order-1 periodic solution both change periodically, with a period of one. The number of phytoplankton in the order-2 periodic solution and the

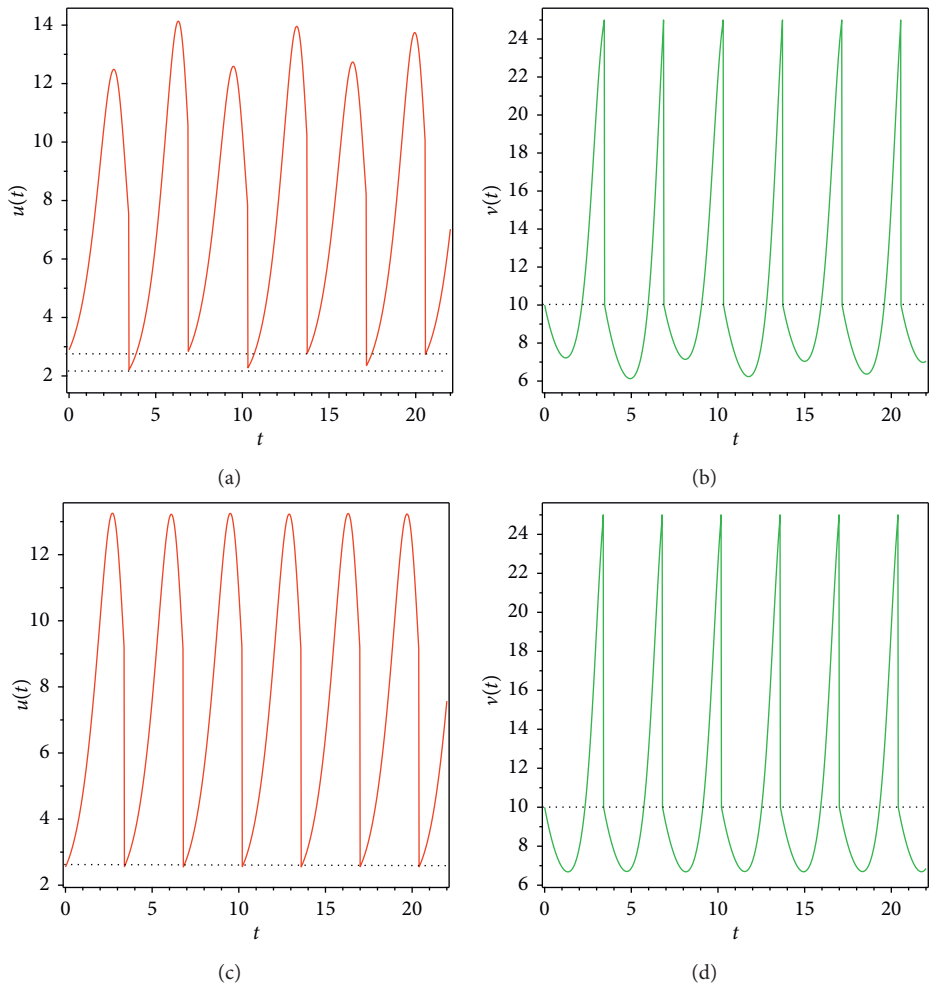

Figure 6: The time series of phytoplankton density (a) and fish density (b) under order-2 periodic solution of Figure 5(b), and the time series of phytoplankton density (c) and fish density (d) under order-1 periodic solution of Figure 5(b).

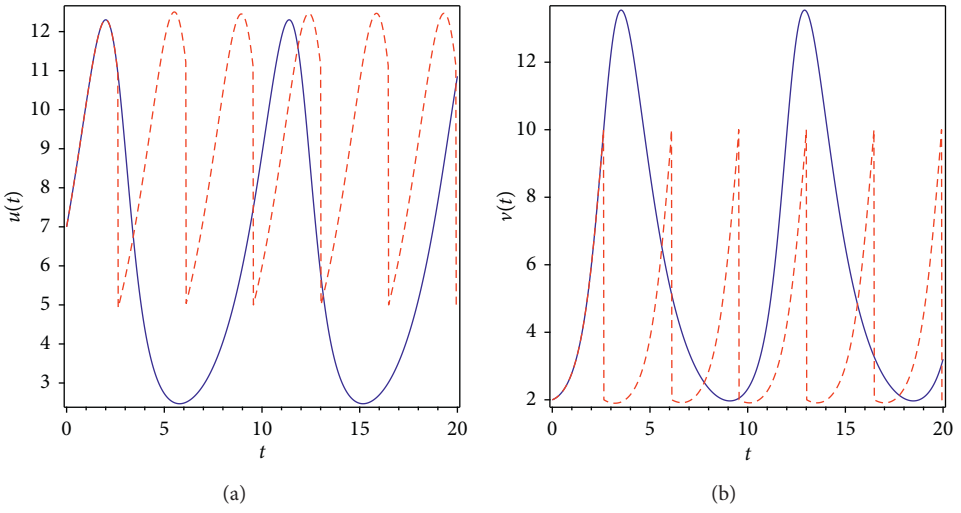

Figure 7: Continued.

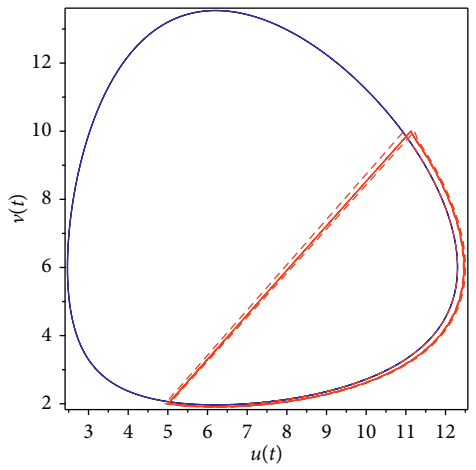

(c)

Figure 7: The time series of phytoplankton density (a), fish density (b), and phase portrait (c) starting from (7,2): $r = 1.444$, $\alpha = 0.1$, $\beta = 0.15$, $d = 0.5$, $a = 0.5$, $b = 1$, $\delta = 0.8$, $\gamma = 1$, $H = 10$, $\theta = 0.01$, and $\tau = 17.36$.

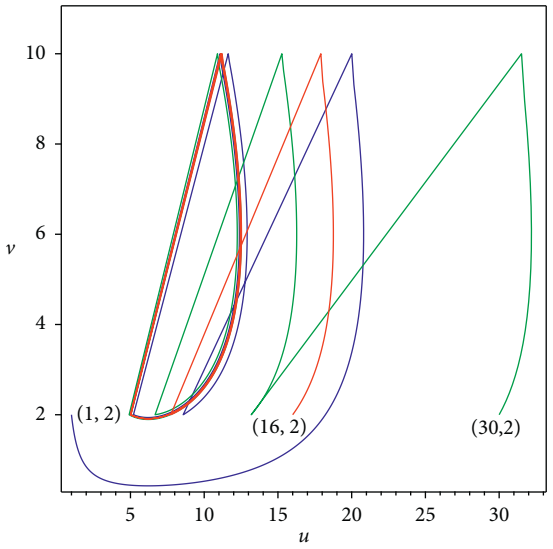

Figure 8: The path curve of system (2) starting from the points (1,2), (16,2), and (20,2), where $r = 0.6$, $\alpha = 0.1$, $\beta = 0.15$, $d = 0.5$, $a = 0.5$, $b = 1$, $\delta = 0.8$, $\gamma = 1$, $H = 10$, $\theta = 0.01$, and $\tau = 17.36$.

order-1 periodic solution are both changing periodically, in which the number of plankton in the order-2 periodic solution has a period of two. The period of the number of phytoplankton in the order-1 periodic solution is one.

In Figure 7, the blue and red lines indicate the trajectory of the system with or without pulses. This shows that the number of phytoplankton and fish can be kept in a stable range.

As can be revealed in Figure 8, different initial points will eventually converge to the same order-1 periodic solution and tend to be stable. This indicates the global asymptotic stability of the order-1 periodic solution.

6. Conclusion

How to rationally develop and utilize fishery resources has become an essential issue for the sustainable development of lake resources. In this paper, we introduce the impulse feedback control into the phytoplankton-fish model. It is of great significance to study the dynamics of phytoplankton and fish.

Compared with [1], we use the Poincare map as a tool to give a more comprehensive qualitative analysis and to prove the dynamics of the phytoplankton-fish model, for example, the necessary and sufficient conditions for the global asymptotic stability of the order-1 periodic solution and the existence conditions of the order-k ($k \geq 2$) periodic solution.

For the biological significance, the order-k ($k \geq 1$) periodic solution of system with state impulsive feedback control indicates that the number of phytoplankton and fish populations can maintain periodic oscillations under certain conditions with proper capture of fish, that is, the number of phytoplankton and fish can be kept in a stable range. These results have some reference values to the dynamic changes in aquatic ecosystem research of fish and phytoplankton.

Data Availability

The data used to support the findings of this study are available upon request from the corresponding author.

Conflicts of Interest

The authors declare that they have no conflicts of interest.

Acknowledgments

This work was supported by the National Natural Science Foundation of China (no. 11371230), Shandong Provincial Natural Science Foundation of China (no. ZR2019MA003), SDUST Research Fund (no. 2014TDJH102), and Joint Innovative Center for Safe and Effective Mining Technology and Equipment of Coal Resources, SDUST Innovation Fund for Graduate Students (no. SDKDYC170225).

References

[1] Z. Zhao, L. Pang, and X. Song, "Optimal control of phytoplankton-fish model with the impulsive feedback control," *Nonlinear Dynamics*, vol. 88, no. 3, pp. 2003–2011, 2017.

[2] H. Guo, L. Chen, and X. Song, "Geometric properties of solution of a cylindrical dynamic system with impulsive state feedback control," *Nonlinear Analysis: Hybrid Systems*, vol. 15, pp. 98–111, 2015.

[3] H. Cheng and T. Zhang, "A new predator-prey model with a profitless delay of digestion and impulsive perturbation on the prey," *Applied Mathematics and Computation*, vol. 217, no. 22, pp. 9198–9208, 2011.

[4] Y. Wang, M. Zhao, X. Pan, and C. Dai, "Dynamic analysis of a phytoplankton-fish model with biological and artificial control," *Discrete Dynamics in Nature and Society*, vol. 10, 2014.

[5] H. T. Sun and Y. Tian, "Continuously harvesting of a phytoplankton-zooplankton system with Holling I functional response," *Applied Mechanics and Materials*, vol. 595, pp. 277–282, 2014.

[6] Y. Wang, W. Jiang, and H. Wang, "Stability and global hopf bifurcation in toxic phytoplankton-zooplankton model with delay and selective harvesting," *Nonlinear Dynamics*, vol. 73, no. 1-2, pp. 881–896, 2013.

[7] Y. Tian, S. Tang, and R. A. Cheke, "Nonlinear state-dependent feedback control of a pest-natural enemy system," *Nonlinear Dynamics*, vol. 94, no. 3, pp. 2243–2263, 2018.

[8] F. Zhu, X. Meng, and T. Zhang, "Optimal harvesting of a competitive n-species stochastic model with delayed diffusions," *Mathematical Biosciences and Engineering*, vol. 16, no. 3, pp. 1554–1574, 2019.

[9] Z. Jiang and X. Bi, "Global hopf bifurcation of a delayed phytoplankton-zooplankton system considering toxin producing effect and delay dependent coefficient," *Mathematical Biosciences and Engineering*, vol. 16, no. 5, pp. 3807–3829, 2019.

[10] Y. Tang, M. Yuen, and L. Zhang, "Double wronskian solutions to the $(2+1)$-dimensional broer-kaup-kupershmidt equation," *Applied Mathematics Letters*, vol. 105, p. 106285, 2020.

[11] H. Liu and H. Cheng, "Dynamic analysis of a prey-predator model with state-dependent control strategy and square root response function," *Advances in Difference Equations*, vol. 2018, no. 1, p. 63, 2018.

[12] T. Feng, Z. Qiu, and X. Meng, "Analysis of a stochastic recovery-relapse epidemic model with periodic parameters and media coverage," *Journal of Applied Analysis and Computation*, vol. 9, no. 3, pp. 1–15, 2019.

[13] G. Liu, Z. Chang, and X. Meng, "Asymptotic analysis of impulsive dispersal predator-prey systems with markov switching on finite-state space," *Journal of Function Spaces*, vol. 2019, p. 18, 2019.

[14] D. Li, H. Cheng, and Y. Liu, "Dynamic analysis of beddington-deangelis predator-prey system with nonlinear impulse feedback control," *Complexity*, vol. 10, 2019.

[15] J. Wang, H. Cheng, H. Liu, and Y. Wang, "Periodic solution and control optimization of a prey-predator model with two types of harvesting," *Advances in Difference Equations*, vol. 2018, no. 1, p. 41, 2018.

[16] L. Zhang, P. Yuan, J. Fu, and C. M. Khalique, "Bifurcations and exact traveling wave solutions of the zakharov-rubenchik equation," *Discrete Continuous Dynamical Systems-S*, vol. 10, pp. 1–13, 2018.

[17] Z. Shi, H. Cheng, Y. Liu, and Y. Wang, "Optimization of an integrated feedback control for a pest management predator-prey model," *Mathematical Biosciences and Engineering*, vol. 16, no. 6, pp. 7963–7981, 2019.

[18] Y. Li, Y. Li, Y. Liu, and H. Cheng, "Stability analysis and control optimization of a prey-predator model with linear feedback control," *Discrete Dynamics in Nature and Society*, p. 12, 2018.

[19] Y. Wang, H. Cheng, and Q. Li, "Dynamic analysis of wild and sterile mosquito release model with Poincaré map," *Mathematical Biosciences and Engineering*, vol. 16, no. 6, pp. 7688–7706, 2019.

[20] F. Wang, B. Chen, Y. Sun, Y. Gao, and C. Lin, "Finite-time fuzzy control of stochastic nonlinear systems," *IEEE transactions on cybernetics*, vol. 15, 2010.

[21] T. Feng and Z. Qiu, "Global analysis of a stochastic TB model with vaccination and treatment," *Discrete & Continuous Dynamical Systems—B*, vol. 24, no. 6, pp. 2923–2939, 2019.

[22] F. Liu, "Continuity and approximate differentiability of multisublinear fractional maximal functions," *Mathematical Inequalities & Applications*, vol. 21, no. 1, pp. 25–40, 2018.

[23] F. Wang and X. Zhang, "Adaptive finite time control of nonlinear systems under time-varying actuator failures," *IEEE Transactions on Systems, Man, and Cybernetics: Systems*, vol. 10, 2009.

[24] Y. Li, H. Cheng, J. Wang, and Y. Wang, "Dynamic analysis of unilateral diffusion gompertz model with impulsive control strategy," *Advances in Difference Equations*, vol. 2018, no. 1, p. 32, 2018.

[25] H. Qi, X. Leng, X. Meng, and T. Zhang, "Periodic solution and ergodic stationary distribution of seis dynamical systems with active and latent patients," *Qualitative Theory of Dynamical Systems*, vol. 10, 2011.

[26] L. Zhang, Y. Shi, and M. Han, "Smooth and singular traveling wave solutions for the serre-green-naghdi equations," *Discrete Continuous Dynamical Systems-S*, vol. 2018, p. 1, 2018.

[27] J. Wang, H. Cheng, X. Meng, and B. S. A. Pradeep, "Geometrical analysis and control optimization of a predator-prey model with multi state-dependent impulse," *Advances in Difference Equations*, vol. 2017, no. 1, p. 252, 2017.

[28] Z. Shi, H. Cheng, Y. Liu, and Y. Li, "A cydia pomonella integrated management predator-prey model with smith growth and linear feedback control," *IEEE Access*, vol. 7, pp. 126066–126076, 2019.

[29] J. Yang and Y. Tan, "Effects of pesticide dose on Holling II predator-prey model with feedback control," *Journal of Biological Dynamics*, vol. 12, no. 1, pp. 527–550, 2018.

[30] L. Xia, T. Zhang, X. Meng, and T. Zhang, "Turing-hopf bifurcations in a predator-prey model with herd behavior, quadratic mortality and prey-taxis," *Physica A: Statistical Mechanics and Its Applications*, vol. 496, pp. 446–460, 2018.

[31] M. Chi and W. Zhao, "Dynamical analysis of multi-nutrient and single microorganism chemostat model in a polluted environment," *Advances in Difference Equations*, vol. 2018, no. 1, p. 120, 2018.

[32] Z. Jiang, W. Zhang, J. Zhang, and T. Zhang, "Dynamical analysis of a phytoplankton-zooplankton system with harvesting term and holling III functional response," *International Journal of Bifurcation and Chaos*, vol. 28, no. 13, p. 1850162, 2018.

[33] F. Wang, Z. Liu, Y. Zhang, and C. L. P. Chen, "Adaptive finite-time control of stochastic nonlinear systems with actuator failures," *Fuzzy Sets and Systems*, vol. 374, pp. 170–183, 2019.

[34] Y. Lv, R. Yuan, and Y. Pei, "A prey-predator model with harvesting for fishery resource with reserve area," *Applied Mathematical Modelling*, vol. 37, no. 5, pp. 3048–3062, 2013.

[35] C. Liu and P. Liu, "Complex dynamics in a harvested nutrient-phytoplankton-zooplankton model with seasonality," *Mathematical Problems in Engineering*, vol. 10, 2014.
[36] L. Zhao, L. Chen, and Q. Zhang, "The geometrical analysis of a predator-prey model with two state impulses," *Mathematical Biosciences*, vol. 238, no. 2, 2010.
[37] Y. Tian, S. Tang, and R. A. Cheke, "Nonlinear state-dependent feedback control of a pest-natural enemy system," *Nonlinear Dynamics*, vol. 94, no. 3, pp. 2243–2263, 2018.
[38] S. Tang, B. Tang, A. Wang, and Y. Xiao, "Holling II predator-prey impulsive semi-dynamic model with complex Poincaré map," *Nonlinear Dynamics*, vol. 81, no. 3, pp. 1575–1596, 2015.
[39] Y. Tian, K. Sun, and L. Chen, "Geometric approach to the stability analysis of the periodic solution in a semi-continuous dynamic system," *International Journal of Biomathematics*, vol. 7, no. 2, pp. 337–163, 2014.
[40] Y. Zhang and F. Wang, "Adaptive neural control of non-strict feedback system with actuator failures and time-varying delays," *Applied Mathematics and Computation*, vol. 362, p. 124512, 2019.